Macromolecules
ARTICLE

Macromolecules **2009**, *42*, 9063–9071 **9063**
DOI: 10.1021/ma901605v

Design of Copolymers with Tunable Randomness Using Discontinuous Molecular Dynamics Simulation

L. Anderson Strickland, Carol K. Hall, and Jan Genzer*

Department of Chemical & Biomolecular Engineering, North Carolina State University, Raleigh, North Carolina 27965-7905

Received July 21, 2009; Revised Manuscript Received September 18, 2009

ABSTRACT: We present the results of discontinuous molecular dynamics simulations of a "coloring" reaction performed on A-type homopolymers having length ranging from 100 to 300 units in implicit solvents. The transformation of selected A-type monomers to B-type units along the macromolecule produces A_{1-x}-*co*-B_x random copolymers, where x is the mole fraction of B (= degree of "coloring"). We demonstrate that for a fixed A−B interaction strength the comonomer distribution of A and B units in A_{1-x}-*co*-B_x can be tuned to range from "purely random" to "random−blocky" by adjusting both the degree of "coloring" and the solubility of the A and B segments with respect to the implicit solvent. In general, increasing the solubility of the A-type homopolymer or the degree of coloring results in a decrease in blockiness in the comonomer distribution. In addition, decreasing the solubility of the B species in the implicit solvent increases the tendency of the $A_{1-x}B_x$ copolymer to form "random−blocky" sequences.

Introduction

Copolymers are macromolecules containing at least two distinct chemical monomer units, say A and B. Depending on the distribution of A and B units along the chain, we distinguish among diblock (...−A−A−B−B−...), triblock (...−A−A−B−...−B−A−A−...), alternating (...−A−B−A−B−...), blocky (...−$(A)_n$−$(B)_m$−...), or random (...−A−B−B−A−A−A−B−...) copolymers. While some copolymers possess an ordered sequence distribution of monomers, random copolymers (RCPs), A-*co*-B, represent a special class of copolymers, which possess a disordered sequence distribution of A and B units. Over the past few decades, a series of papers have been published which established that tuning the copolymer chemical composition and comonomer sequence distribution profoundly affects the characteristics of random copolymers.[1−14] Of those characteristics intrinsic to the polymer, most work performed to date addressed the role of the chemical composition. By judiciously choosing the A and B chemical species, RCPs have the potential to act as polymer blend compatibilizers[15−17] or adhesion promoters.[6−8,18−21] Recent efforts[22] have concentrated on investigating the role of the monomer distribution along the RCP backbone in controlling the polymer's physicochemical characteristics such as the coil-to-globule transition temperature and conformation. To that end, Chakraborty and co-workers investigated the bulk properties of RCPs and observed that the tunability of the polymer's blockiness may endow RCPs with the ability to act as pattern recognition agents for similarly patterned surfaces.[23−25]

Having good control over both the chemical composition and the comonomer sequence distribution in RCPs is essential for many applications. While tailoring the content of A and B in RCP is relatively straightforward, adjusting the distribution of monomers along the polymer backbone is not. Progress in this direction was recently made by Khokhlov and co-workers, who designed an elegant computational approach to tune the blockiness of RCPs.[10−12,26−28] Their approach involves collapsing an A homopolymer in a poor solvent and then "coloring" the outer exposed shell of the resulting globule with B species.[26,27] Khokhlov and co-workers reported that the A-homopolymers that were collapsed before "chemically coloring" exhibited random−blocky monomer sequences since only the monomers present on the periphery of the collapsed coil underwent chemical modification. The resulting sequence was called a "protein-like" copolymer (PLC). In contrast, the A homopolymers that were fully expanded during the coloring process exhibited a random distribution of the "colored" species.

It is of interest to consider how differences in the solubility of a homopolymer A and colored monomer B affect the sequence of the resulting copolymer. One would expect that as the coloring reaction evolves, solubility of the newly created monomers along the A-*co*-B copolymer affects the chain conformation and ultimately the distribution of the A and B units inside the RCP. To this end, while coloring the A homopolymer with B species that are more soluble in the solvent should result in opening up the chain, B monomers that are less soluble than the A units would move toward the center of the collapsed polymer. In their initial work Khokhlov and co-workers did not examine these questions since the coloring reaction was assumed to be instantaneous (i.e., the parent homopolymer coil was "frozen"). Realizing that the coil's conformation would likely change as the "chemical coloring" proceeded, Semler and Genzer performed computer simulations that explored how variations in the conformation of the parent coil over the course of the coloring reaction affect the comonomer sequence distribution.[29] But they assumed that the solubilities of the colored and noncolored monomers were the same. Later, Khokhlov and collaborators considered how variations in the monomer solubility affect sequence distribution, focusing on the case in which the newly colored monomer exhibits a higher solubility in the solvent than the parent homopolymer.[22] In that case, the originally collapsed coil started to unfold as the coloring progressed, as expected.

As mentioned earlier, there is also the possibility that the colored monomer B will exhibit lower solubility in the solvent

*Corresponding author: E-mail Jan_Genzer@ncsu.edu, Fax +1-919-551-2069.

Published on Web 09/30/2009

than the original "uncolored" monomer A. This appears to have been the case in recent experimental work by Genzer and co-workers, who carried out a coloring reaction by brominating parent polystyrene coils in selective solvents.[30−32] Bromination of styrene (S) monomers performed in chlorinated alkanes, such as 1-chlorodecane (CD) and 1-chlorododecane (CDD), led to poly(styrene-*co*-4-bromostyrene) copolymers (PBr_xS), where x is the mole fraction of 4-bromostyrene (4-BrS) units, which contained solvent-dependent comonomer distributions. As expected based on Khokhlov's original ideas, bromination in a good solvent (CD) resulted in a random distribution of S and 4-BrS, while bromination in a poor solvent (CDD) produced a random−blocky distribution of S and 4-BrS, as deduced by electro-optical Kerr effect measurements.[30−32] In addition, the colored (brominated) monomers in these experiments appeared to exhibit lower solubility than the uncolored (styrene) monomers. Evidence for this hypothesis comes from preliminary (unpublished) in situ small-angle neutron scattering data, indicating that the globule may have inverted over the course of the bromination process. Genzer and co-workers concluded that the level of blockiness present in their final PBr_xS RCP was related not only to the impact of the solvent quality on the parent (noncolored) homopolymer but also to the difference between the solubility of the colored and noncolored monomers which triggered conformational changes during the bromination process. While limited experimental evidence for this interpretation exists,[33] a complete understanding of how solubility differences between colored and uncolored monomers affect sequence blockiness can only be deduced by following the "coloring" reaction using molecular modeling. That is the motivation for the work presented here.

In this paper, we present the results of discontinuous molecular dynamics (DMD) simulations of polymer "coloring" reactions with special focus on the case in which the colored monomers have different solubility than the parent homopolymer. A system of polymer molecules, modeled as chains containing 100−300 square-well monomers of A type (corresponding to styrene), is allowed to equilibrate at a selected reduced temperature. After equilibration, athermal reactant particles are placed in the simulation box. When the reactant particles come in contact with A-type monomers, the monomer is "colored" to become a B-type monomer (corresponding to 4-BrS). This "coloring" reaction is carried out until a desired number of the parent monomers is colored. Since the solvent in our simulations is implicit, the solubility of A- and B-type monomers is adjusted by varying the A−A and B−B interaction strengths. The ratio of B−B interaction strength to A−A interaction strength ($R_{BA} = |\varepsilon_{BB}|/|\varepsilon_{AA}|$) is varied from 0.5 to 10.0. In this manner, the newly created B unit can be modeled as either more or less soluble than A. Interactions between nonbonded A and B units along the chain are modeled as athermal, i.e., $\varepsilon_{AB} = 0$. In a separate publication, we address the effect of varying ε_{AB} on the system behavior.[34] Finally, the distribution of A and B units along the polymer chain is calculated in order to determine the effect of solubility and chain length on comonomer distribution in the A-*co*-B copolymer.

Highlights of this work are as follows. The sequence distribution of A and B species in the A-*co*-B copolymer is affected by the interaction strengths acting between the A−A and B−B monomers. At low $kT/|\varepsilon_{AA}|$ the homopolymers adopt a tight globule conformation; at high $kT/|\varepsilon_{AA}|$ the coils expand. The boundary between the two regimes defines the coil-to-globule transition temperature, T^*_θ. The conformation of the parent homopolymer dictates which part of the homopolymer is available to the reactant for coloring; good solvents expose the entire length of the chain to the reactant while poor solvents expose only the outer shell of the globule. In general, when the solubility of the B monomers is not the same as the A monomers (i.e., $\varepsilon_{AA} \neq \varepsilon_{BB}$), the chain conformation changes during the coloring reaction by either expanding (when B is more soluble than A) or contracting (when B is less soluble than A). We find that there exists a minimum degree of "coloring" before substantial chain reconfiguration can take place; typically, reconfiguration requires a minimum of 20% conversion of A to B. For high values of R_{BA} (i.e., very low B solubility), the B monomers tend to move toward the center of the globule, causing the globule to invert. Lastly, we show how to choose the variables governing the copolymer bromination process (system temperature, R_{BA}, and percent of "coloring") to produce copolymers of specific blockiness. In general, low $kT/|\varepsilon_{AA}|$ (low kT and/or high $|\varepsilon_{AA}|$) and good B solubility lead to the formation of tight globules and hence produce A-*co*-B copolymers with increased tendency toward random−blocky comonomer distribution. In contrast, high $kT/|\varepsilon_{AA}|$ (high kT and/or low $|\varepsilon_{AA}|$) plus good B solubility leads to extended homopolymer conformations, which produce A-*co*-B copolymers with random comonomer distribution. More interesting and somewhat unexpected behavior occurs when the solubility of B is poor compared to that of A. One might expect that in cases of poor B solubility the copolymer would contract in size during the coloring process; instead, at $kT/|\varepsilon_{AA}| < T^*_\theta$ we observe an initial swelling of the copolymer as B monomers move into the globule away from the solvent. We also noted cases of blocky copolymers formed in good solubility conditions ($kT/|\varepsilon_{AA}| \gg T^*_\theta$) due to poor B solubility; the formation of subglobules at the chain ends mimicked low solubility.

The remainder of the paper is organized as follows. First, we describe the model and the simulation method used to model the "coloring" process. Next, we present the results from our simulations and provide a discussion of these results. We conclude with a short summary and discussion.

Molecular Model and Simulation Method

The model used to simulate polymers has been previously described;[35−37] thus, only the highlights and any deviations from previous work follow. The polymer molecules are modeled as freely jointed chains comprising monomers that interact via a square-well potential. The potential energy for nonbonded monomer−monomer interactions can be written as

$$U(r) = \begin{cases} \infty & r < \sigma \\ -\varepsilon_{ij} & \sigma \le r \le \lambda\sigma \\ 0 & r > \lambda\sigma \end{cases} \quad (1)$$

where σ denotes the monomer diameter, λ is the width of the square-well interaction, and ε_{ij} is the depth of the square well acting between monomers i and j. In this work, σ and λ are set to 1.0 and 1.5, respectively, for all A- and B-type monomers. The diameter of the reactant particles, σ_R, is set to 0.175, and as we are working at a low reactant concentration, we chose to model the reactant−reactant interactions as athermal; thus, λ_R is irrelevant. The interaction potential for all unlike interactions is set to zero, i.e., $\varepsilon_{AB} = 0$. The interaction potential for all like interactions (i.e., ε_{AA} and ε_{BB}) is varied. The simulation method used here is discontinuous molecular dynamics (DMD), a fast alternative to traditional molecular dynamics. Unlike traditional molecular dynamics, which employs a monomer−monomer interaction potential that is a continuous function of their separation (e.g., the Lennard-Jones potential), DMD replaces monomer−monomer interactions with a square well, which incorporates short-range repulsions as well as long-range attractions. The advantage of DMD over traditional molecular dynamics is that monomers need not be moved incrementally at short regularly spaced time steps. Instead, we are only concerned with the

collision time, t_{ij}, at which a monomer reaches a discontinuity in its potential energy, $U(r)$, e.g., when it undergoes core repulsion with another monomer, when it enters/leaves the square-well interaction of another monomer, or when, lacking enough kinetic energy, it remains in a well. Collision times for all monomers in the system are calculated, the minimum collision time for the system, t_c, is chosen, and all monomers are advanced forward according to

$$\mathbf{r}_i(t+t_c) = \mathbf{r}_i(t)+\mathbf{v}_i t_c \quad (2)$$

where $\mathbf{r}_i$ and $\mathbf{v}_i$ represent the ith monomer's position and velocity, respectively. At this point, two monomers collide, their new postcollision velocities are calculated, and this process is continued.

The length of the bonds between the monomers along the polymer chain fluctuates freely over the range $\sigma(1 \pm \delta)$ where δ is a small number.[38] This treatment makes the average bond length between neighboring monomers equal to σ, which is close in architecture to tangentially connected monomers. Nonbonded monomers along a chain interact with the same potential as monomers on different chains. The solvent is modeled implicitly since explicit treatment would require the addition of solvent molecules and is computationally intensive. The solubility of our polymers in the implicit solvent is represented indirectly by the value of the ratio of the system reduced temperature, kT, and the potential of mean force between the monomers, ε_{AA}, i.e., $kT/|\varepsilon_{AA}|$. For relatively low values of $kT/|\varepsilon_{AA}|$ (say 1.0), monomers lack the energy necessary to escape the square-well interaction; here the polymers adopt compact configurations which corresponds to low solubility. In contrast, high values of $kT/|\varepsilon_{AA}|$ (say above 4.0) bestow sufficient kinetic energy to the monomers for them to escape square-well interaction with one another; as a result, the polymers adopt extended configurations which corresponds to good solubility. Thus, the solubility of the homopolymers is measured by $kT/|\varepsilon_{AA}|$. This implicit solvent model saves us the extra computational expense associated with introducing solvent molecules explicitly into the simulation.

The temperature is held constant throughout the simulation. This is accomplished through the use of an Andersen thermostat, which allows the temperature to fluctuate about the average value, kT.[39] A ghost particle having no position or velocity is created with a random collision time, t_g. When, during the course of the simulation, the chosen minimum collision time equals or exceeds t_g, a monomer is selected at random and its velocity is recalculated according to a Gaussian distribution on kT. The ghost particle's collision time is reset and normal collisions resume. System temperature fluctuations are allowed but should be neither too big nor too small. See ref 40 for further discussion on this topic.

In order to simulate the experimental coloring process, i.e., the bromination of polystyrene, a single homopolymer chain is placed in a box of fixed volume (typical box length = 150σ), where σ, the monomer diameter, is set to 1. The polymer is equilibrated for several hundred million collisions at the chosen kT. Next, the box is randomly filled with reactant particles at a ratio of three reactant particles per monomer unit. This is the same ratio that was used by Jhon and co-workers in their experimental studies of bromination of polystyrene chains.[30,31] A typical reactant particle packing fraction, i.e., volume of reactant particles divided by the volume of the box, is < 0.0001, which we calculate knowing the number of reactant particles (say 3×100) and the volume of the simulation box ($150^3\sigma^3$). Because the reactant particle packing fraction is well below 1%, collisions between reactant particles are rare enough that they are not expected to affect the coloring process. For this reason, we model the reactant−reactant interactions as athermal. Upon contact between an A monomer and a reactant particle, the A monomer is "colored" and converted from an A species into a B species. The reactant particle is removed and then placed back in the box at a random location to maintain a constant reactant particle packing fraction. This event corresponds in real experiments to the bromination of styrene by Br_2 to create 4-BrS.[30,31] As we do not require the reactant particle to approach the chain at a specific angle to the backbone, all A reactant interactions are considered effective and all A → B conversions are accepted. The reaction does not change the volume of the monomer; thus $\sigma_A = \sigma_B$. The chain moves according to Newton's equation of motion throughout the coloring process. The coloring reaction is run until the chain is composed of at least 60% B particles. Since we are interested not only in the A-*co*-B copolymer distribution but also the effects of coloring on the conformation of the chain, data are collected at regularly spaced collision numbers on the polymer's mean-square radius of gyration, $\langle R_g^2 \rangle$, defined as

$$\langle R_g^2 \rangle = \frac{\langle \sum_{(i)} (\mathbf{r}_i - \mathbf{r}_{CM})^2 \rangle}{N} \quad (3)$$

where $\mathbf{r}_i$ is the ith monomer position and $\mathbf{r}_{CM}$ is the center of mass for the chain; the summation is averaged over all chains in the system.

Coloring reaction simulations on chains of length (N) ranging from 100 to 300 monomers were performed at $kT/|\varepsilon_{AA}|$ ranging from 0.04 to 8.0 to explore poor, theta, and good solvent conditions. The ratio of the B−B interaction strength to the A−A interaction, $R_{BA} = |\varepsilon_{BB}|/|\varepsilon_{AA}|$, was set to 0.5, 1.0, 5.0, and 10.0. Each system was equilibrated over ~100 million collisions in a box of size $L = 150\sigma$. Subsequently, $3N$ reactant particles were added; each coloring reaction was run at least three times for each set of system conditions to produce average data at each temperature.

Results and Discussion

We first located the theta temperature for our parent homopolymer systems. Others have shown using lattice Monte Carlo computer simulations[41] that the theta temperature (T_θ) for a long polymer chain with interactions of strength of $\varepsilon_{AA} = -1.0$ occurs at $T^* \approx 3$. At $kT/|\varepsilon_{AA}| < T^*_\theta$, corresponding to poor solvent conditions, polymers adopt a globule conformation, while at $kT/|\varepsilon_{AA}| > T^*_\theta$, representing good solvent conditions, polymers extend out in a coil conformation. This trend was confirmed in our simulations, as seen from the radius of gyration data for 300-mers in Figure 1. Polymers at temperatures up to $kT/|\varepsilon_{AA}| \approx 2$ adopt a globule formation (with $\langle R_g^2 \rangle$ values less than 10% of the chain's length) while polymers at temperatures at or above $kT/|\varepsilon_{AA}| \approx 6$ extend in coil conformations. Thus, for our system, the coil-to-globule transition and hence the theta temperature, T^*_θ, occurs at around $kT/|\varepsilon_{AA}| \approx 3$.

While the conformation of the parent homopolymer is affected only by the value of $kT/|\varepsilon_{AA}|$, the conformation of the $A_{1-x}B_x$ copolymer, where x is the "degree of coloring", depends on $kT/|\varepsilon_{AA}|$, R_{BA}, and N. We demonstrate that the solubility difference between B and A, as measured by R_{BA}, alters the conformation of the polymer; in addition, the polymer's ability to expand or contract is directly related to the polymer length. In Figure 2, we plot the mean-square radius of gyration as a function of degree of coloring for chain lengths ranging from 100 to 300. For this analysis, we set $kT/|\varepsilon_{AA}| = 0.2$ and $R_{BA} = 10.0$, which is equivalent to poor solvent conditions for the parent homopolymer and extremely poor solubility for B. In general, the radius of gyration increases as the degree of polymerization, N, increases; this result is trivial. Of greater interest, however, is the change in the radius of gyration as a function of the degree of coloring *relative* to the radius of gyration of the uncolored parent homopolymer. For the

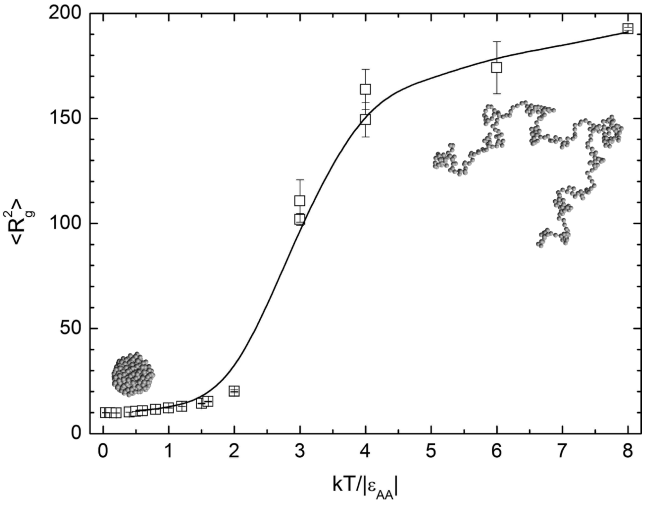

Figure 1. Mean-square radius of gyration of a 300-mer containing monomers of type A as a function of $kT/|\varepsilon_{AA}|$. The line is meant to guide the eye. The insets denote the conformations of the low-temperature globule ($kT/|\varepsilon_{AA}| = 0.2$) and high-temperature coil ($kT/|\varepsilon_{AA}| = 8.0$).

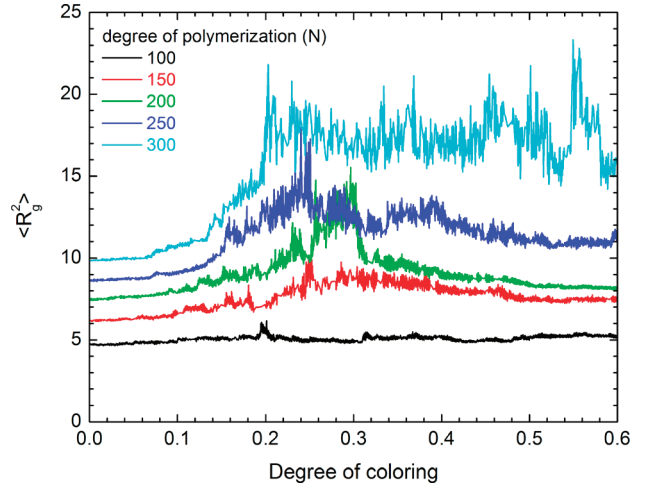

Figure 2. Mean-square radius of gyration as a function of the degree of coloring (i.e., the mole fraction of B units, x, in $A_{1-x}B_x$) for polymers of chain length ranging from 100 to 300 at R_{BA} ($= |\varepsilon_{BB}|/|\varepsilon_{AA}|$) = 10.0 and $kT/|\varepsilon_{AA}| = 0.2$ (poor solvent).

shortest chains ($N = 100$), $\langle R_g^2 \rangle$ is independent of the degree of coloring. Increasing N to 150 results in a modest increase of $\langle R_g^2 \rangle$ at ≈30% coloring. For all systems above chain length 150, $\langle R_g^2 \rangle$ values spike rapidly at ≈20% coloring, clearly indicating that the newly generated B segments affect the overall mean radius of gyration of the polymer. These results reveal that the chain's conformation is a function not only of $kT/|\varepsilon_{AA}|$ (as stated previously) but also of the amount of B and chain length.

One would expect R_{BA} to strongly influence the chain conformation and thus the size of the coil. To analyze this, we varied R_{BA} at the longest chain length, $N = 300$, since the strongest conformational changes are expected to occur for the longest chains.[42] The parameter R_{BA} was varied from 0.5 to 10.0 in order to explore cases when the presence of the newly created B units increases ($R_{BA} < 1$) or decreases ($R_{BA} > 1$) the solubility of the chain. Recall that the value of $kT/|\varepsilon_{AA}|$ determines whether or not the polymer adopts a globular or coil conformation *prior to* the beginning of coloring. Varying R_{BA} allows us to fine-tune the chain conformation *during* the coloring process and, as will be

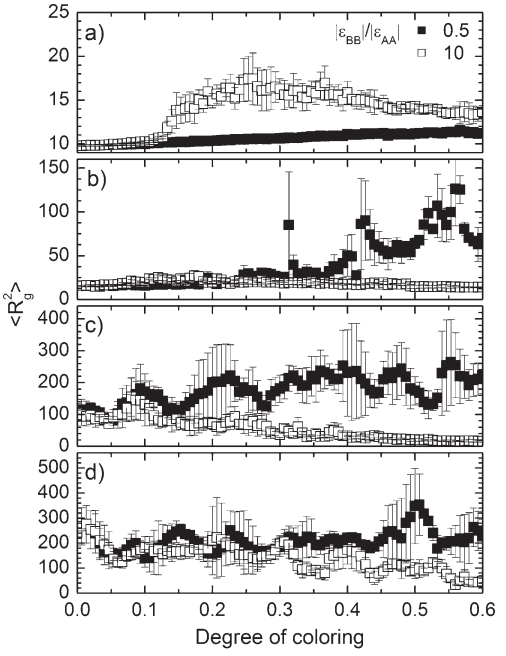

Figure 3. Mean-square radius of gyration as a function of the degree of coloring, x (i.e., the mole fraction of B units, x, in $A_{1-x}B_x$) for 300-mers at R_{BA} ($= |\varepsilon_{BB}|/|\varepsilon_{AA}|$) = 0.5 (closed symbols) and 10 (open symbols) and various reduced temperatures ($kT/|\varepsilon_{AA}|$) equal to (a) 0.2, (b) 1.6, (c) 3.0, and (d) 8.0. The error bars were obtained by averaging over three simulation runs.

demonstrated later in the paper, ultimately affects the distribution of the A and B units along the chain. Setting $R_{BA} < 1$ is expected to increase the solubility of the chain and hence lead to an increase of its size. Setting $R_{BA} > 1$ should have the opposite effect and lead to more compact chains.

The value of R_{BA}, however, has a much more complex effect on the size of the chain than one would expect. When $|\varepsilon_{BB}| \gg |\varepsilon_{AA}|$, one might expect the globule size to decrease (extremely poor solubility) with increasing coloring. Instead, as can be seen by examining the data in Figure 2, the globule size increases with increased degree of coloring, an effect which is counterintuitive. As we will explain below, it is the interplay among ε_{AA}, ε_{BB}, and ε_{AB} that governs the final conformation of the random $A_{1-x}B_x$ copolymer. Figure 3 shows the mean-square radius of gyration of $A_{1-x}B_x$ as a function of the degree of coloring for 300-mers at R_{BA} equal to 0.5 (close symbols) and 10.0 (open symbols), values corresponding to relatively good solubility and poor B solubility, respectively. Note that the $\langle R_g^2 \rangle$ values at a given $kT/|\varepsilon_{AA}|$ are the same for each R_{BA} before coloring takes place; they correspond to the $\langle R_g^2 \rangle$ depicted in Figure 1. Small apparent discrepancies between the data in Figures 1 and 3 are due to the steep rise in $\langle R_g^2 \rangle$ at very small degrees of coloring that are not resolved in Figure 3 due to the plotting range. The data are taken at four values of $kT/|\varepsilon_{AA}|$: 0.2, 1.6, 3.0, and 8.0. There are several trends worth noting. At $kT/|\varepsilon_{AA}|$ below T^*_θ (i.e., 0.2 and 1.6), the mean radius of gyration of the globule prior to coloring is relatively small compared to the chain length (roughly $\langle R_g^2 \rangle$ values of 9 and 11, respectively). At $kT/|\varepsilon_{AA}| = 3.0$ (or T^*_θ), $\langle R_g^2 \rangle$ prior to coloring increases to 100, and at $kT/|\varepsilon_{AA}| = 8.0$, $\langle R_g^2 \rangle$ reaches nearly 300 prior to any coloring. Thus, the globule size of the parent homopolymer is a strong function of $kT/|\varepsilon_{AA}|$. Furthermore, the parent homopolymer globule determines which monomers are available for coloring; thus, we can infer that a large fraction of the chain segments are inaccessible at low $kT/|\varepsilon_{AA}|$ while the majority of the chain segments are exposed at high $kT/|\varepsilon_{AA}|$.

Looking at the change in $\langle R_g^2 \rangle$ in Figure 3 for the copolymer $A_{1-x}B_x$ as a function of the degree of coloring (x), we can infer how the solubility of the newly formed B monomers affects the globule size during the coloring process. At $kT/|\varepsilon_{AA}| = 0.2$, $\langle R_g^2 \rangle$ values for the two systems $R_{BA} = 0.5$ and 10.0 are roughly equivalent over the range of $0 \leq x \leq 0.15$. At this point, $\langle R_g^2 \rangle$ for the $R_{BA} = 10.0$ system increases rapidly, nearly doubling in value. Because of the low solubility of B and $\varepsilon_{AB} = 0.0$ (athermal), the B monomers have moved to the center of the globule away from the implicit solvent (as will be documented later in the paper), forcing the A monomers outward, thereby increasing $\langle R_g^2 \rangle$; thus, we can infer that the system with poor B solubility has inverted during coloring. This effect reaches a maximum between $x = 0.2$ and 0.3. With additional coloring, the globule shrinks back toward the original size as B monomers formed on the outside are attracted to the growing B-core. By comparison, $\langle R_g^2 \rangle$ for $R_{BA} = 0.5$ at $kT/|\varepsilon_{AA}| = 0.2$ increases no more than 10% over in the entire range of coloring. The B monomers formed in the good B solubility case are believed to have remained on the surface of the globule. This will be discussed in more detail below when we introduce Figure 4.

The main reason for B monomer migration toward the center when $R_{BA} \gg 1$ is the relative change in solubility during the coloring process. While the coloring process begins at low or high homopolymer solubility as determined by the value of $kT/|\varepsilon_{AA}|$, the formation of B monomers alters this solubility. In Figure 3a, when $kT/|\varepsilon_{AA}| = 0.2$, the system begins as a homopolymer globule in a poor solvent and, regardless of the solubility of B, remains in poor solvent throughout coloring ($\langle R_g^2 \rangle$ is very low for both $R_{BA} = 0.5$ and 10.0 over the investigated range of coloring). In Figure 3b when $kT/|\varepsilon_{AA}| = 1.6$ and $R_{BA} = 10.0$, the B monomers start out on the surface and at $x \approx 0.20$ the globule size expands as B monomers move to the core. As the degree of coloring increases to $x \approx 0.60$ the globule size starts to decrease. The overall change in globule size is minor compared to the change which occurs when $R_{BA} = 0.5$. For $R_{BA} = 0.5$, the globule prior to $x \approx 0.20$ hardly changes shape; the new B monomers are soluble and remain largely on the surface of the globule. At $x \approx 0.40$, however, the globule begins to expand rapidly, and by $x \approx 0.50$, the copolymer $\langle R_g^2 \rangle$ increases 10-fold relative to the original homopolymer size. This behavior can be explained by looking at the reduced temperature for both A *and* B monomers. If we were to allow the A homopolymer to completely convert to a B homopolymer, the new reduced temperature from B's point of view would be $kT/(|\varepsilon_{AA}|/R_{BA}) = 1.6/0.5 = 3.2$, which is above T^*_θ. Thus, as the poor-solvent homopolymer is colored, it begins to expand as if it were in good solvent due to the solubility of B. In essence, the good solubility of B reduces the effective theta temperature of the system *as the chain is being colored.*

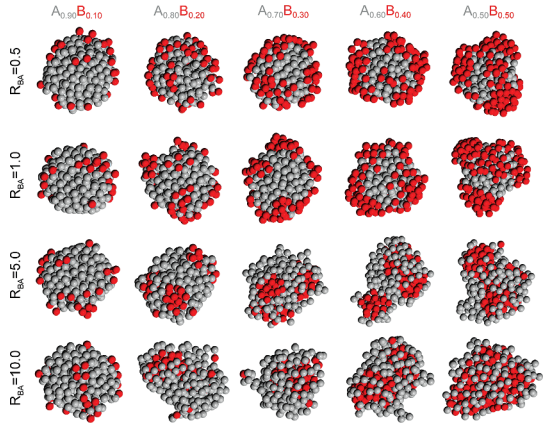

Figure 4. Conformation of a 300-mer $A_{1-x}B_x$ prepared by "coloring" a parent A 300-mer (gray balls) with the coloring species (red balls) to various degrees of coloring, x, ranging from 0 to 0.5 at $kT/|\varepsilon_{AA}| = 0.2$ and $R_{BA} = |\varepsilon_{BB}|/|\varepsilon_{AA}| = 0.5$, 1.0, 5.0, and 10.0.

Next, we investigate the opposite trend, namely, when poor solubility of B increases the effective theta temperate of the system during coloring. When $kT/|\varepsilon_{AA}| = 3.0$ (cf. Figure 3c), both parent homopolymers begin in an expanded conformation. In good B solubility ($R_{BA} = 0.5$), the chain slowly expands 2-fold as x increases from 0 to 0.5. By comparison, in poor solubility ($R_{BA} = 10.0$), the globule size decreases from $\langle R_g^2 \rangle = 100$ to 20 as x increases from 0 to 0.5. Here we note that the effective $kT/|\varepsilon_{AA}|$ relative to B is $kT/(|\varepsilon_{AA}|/R_{BA}) = 0.3$, which is far less than T^*_θ; as such, the chain transforms from coil-to-globule as the chain is colored. In other words, the poor solubility of B increases the effective theta temperature of the system *as the chain is being colored.*

The change in the globule conformation during the coloring process can be extreme. In Figure 3d, we plot $\langle R_g^2 \rangle$ as a function of the degree of coloring for $kT/|\varepsilon_{AA}| = 8.0$. Here the parent homopolymer is fully expanded at the beginning due to very good solvent conditions. The radius of gyration for the good B solubility system ($R_{BA} = 0.5$) does not vary much over the range of coloring; it fluctuates around $\langle R_g^2 \rangle = 200$ for most of the coloring process. In contrast, the chain size in the poor B solubility system ($R_{BA} = 10.0$) is a strong function of degree of coloring: $\langle R_g^2 \rangle \approx 250$ at 0% coloring and decreases to $\langle R_g^2 \rangle \approx 25$ at $x \approx 0.50$. The decrease in globule size is due to the newly created B monomers collapsing inward, away from the implicit solvent. This system ($kT/|\varepsilon_{AA}| = 8.0$, $R_{BA} = 10.0$) will be discussed further in Figure 9.

The results presented in Figure 3 are summarized in Table 1, which shows that the changes in chain conformation during the coloring process can be divided into four major categories, depending on the initial conformation of the parent homopolymer (globule or coil) and the relative solubility of B (more or less soluble). Overall, the development of $\langle R_g^2 \rangle$ with increasing the degree of coloring depends on the interplay among ε_{AA}, ε_{BB}, and ε_{AB}. In the present case when $\varepsilon_{AB} = 0$, strong repulsive interactions between the colored monomer and the solvent (i.e., high $|\varepsilon_{BB}|/|\varepsilon_{AA}|$) drive the colored monomers inward; the increased number of A−B interactions dilutes the attraction between the A−A segments leading to fluctuations in the coil size (i.e., effectively, the attractions between the A−A segments are replaced with the athermal A−B contacts). In a separate publication[34] we address the role of the ε_{AB} interactions in governing the $\langle R_g^2 \rangle$ and the resulting comonomer distributions inside the system.

The model proposed in the original Khokhlov's work, i.e., in which an A-type homopolymer does not change its conformation as the outer surface is colored, is improbable. More specifically, the only case where this model could be justified is when good-solubility B monomers form on the surface of a collapsed parent globule homopolymer (poor solubility) that remains a globule

Table 1. Effect of A and B Solubility on Copolymer Conformation during the Coloring Process

parent conformation	B monomer solubility	change in $\langle R_g^2 \rangle$ upon increasing x
coil (soluble) $kT/\|\varepsilon_{AA}\| > T_\theta$	good $kT/\|\varepsilon_{BB}\| > T_\theta$	minor increase or no change
coil (soluble) $kT/\|\varepsilon_{AA}\| > T_\theta$	poor $kT/\|\varepsilon_{BB}\| < T_\theta$	slow contraction
globule (insoluble) $kT/\|\varepsilon_{AA}\| < T_\theta$	good $kT/\|\varepsilon_{BB}\| > T_\theta$	rapid expansion at $x \approx 0.30$, followed by slow expansion
globule (insoluble) $kT/\|\varepsilon_{AA}\| < T_\theta$	poor $kT/\| < \varepsilon_{BB}\| < T_\theta$	rapid expansion at $x \approx 0.20$, followed by slow collapse

during the coloring process. When the newly formed B monomer has a different solubility than the original A-monomer, the conformation of the chain changes during the coloring process. This could be critical in the design of new copolymers with selected A-*co*-B blockiness, as will be discussed below.

It is useful to understand how the formation of a B-monomer changes the copolymer conformation that the next reactant particle will encounter. Here we describe how the location of the B monomers changes during the coloring process. In Figure 4, we present snapshots of characteristic conformations of $A_{1-x}B_x$ copolymers as a function of the degree of coloring (x) for varying R_{BA} ($= |\varepsilon_{BB}|/|\varepsilon_{AA}|$) at $kT/|\varepsilon_{AA}| = 0.2$, i.e., in a poor solvent system. The degree of coloring increases from left to right, while the solubility of B decreases from top to bottom. In the top row, B is more soluble than A ($R_{BA} = 0.5$), and accordingly all B units (colored red) remain on the outer shell of the globule during the coloring reaction. There is little B−B clustering on the surface as the B units do not tend to associate at this solubility. In the second row, when the solubility of B equals that of A ($R_{BA} = 1$), the B units remain on the surface with little B−B clustering since neither monomer has a preference for like monomers. In the third row, B solubility is worse than A ($R_{BA} = 5.0$). Here the B units initially form on the surface (cf. $A_{0.90}B_{0.10}$) and as the coloring proceeds tend to form islands on the surface because of strong B−B interaction (cf. $A_{0.80}B_{0.20}$). Coloring to 40% (cf. $A_{0.60}B_{0.40}$) distorts that the shape of the globule as the B monomers move toward the center of the copolymer. At 50% coloring (cf. $A_{0.50}B_{0.50}$) B has now formed a nucleus inside the globule. Finally, in the fourth row, for very poor solubility of B ($R_{BA} = 10.0$), relatively little coloring is required (cf. $A_{0.80}B_{0.20}$) for the copolymer to form a distinct B nucleus.

We now return to the observations discussed earlier in Figure 2. Recall that for the short polymers we detected very small variations in $\langle R_g^2 \rangle$ with increasing degree of coloring but for the longer macromolecules we observed substantial increases in $\langle R_g^2 \rangle$ once they reached a "critical" degree of coloring. Results presented in Figures 3 and 4 reveal that for $R_{BA} \gg 1$ the B segments tend to burrow into the globule in order to shield themselves from the solvent. This inversion process (i.e., the tendency of the B units to traverse to the interior of the coil) does not cause substantial variation in coil size for low molecular weight polymers because they are not large enough to shield a portion of the polymer from the solvent. In contrast, the inversion process has a significant impact on the overall size of the macromolecules for high molecular weight polymers ($N > 150$) which are large enough to shield a portion of the polymer from the solvent; thus, high-MW polymers are capable of adopting more compact globular conformations.

Recall that a main thrust of this work is to understand how varying the molecular parameters of the system (i.e., $kT/|\varepsilon_{AA}|$, $\varepsilon_{BB}/\varepsilon_{AA}$, and x) affects the distribution of A and B units along the $A_{1-x}B_x$ copolymer. To that end, it is necessary to quantify the "blockiness" or "randomness" of the polymer. In Figure 5, we show a 300-mer of composition $A_{0.5}B_{0.5}$ in an extended conformation at $kT/|\varepsilon_{AA}| = 8.0$. On the basis of the earlier work by Khokhlov et al.,[26] we assign the values 1 and −1, denoting the units A and B, respectively, to the monomers. What results when we plot these values as a function of the monomer location along the macromolecule is a "barcode" plot (seen in the bottom of Figure 5). Barcode plots of a blocky $A_{1-x}B_x$ copolymer would display wide black and white patches while plots of truly random copolymers would display many thin black and white strips. The utility of this type of plot lies in its ability to illustrate the differences between polymers with the same percent coloring but different comonomer distributions. Figure 6 shows barcode plots for $A_{0.5}B_{0.5}$ at $kT/|\varepsilon_{AA}|$ equal to (a) 0.2, (b) 0.6, (c) 0.8, and (d) 1.2 for 300-mers, all having the same B-solubility ($R_{BA} = 5.0$).

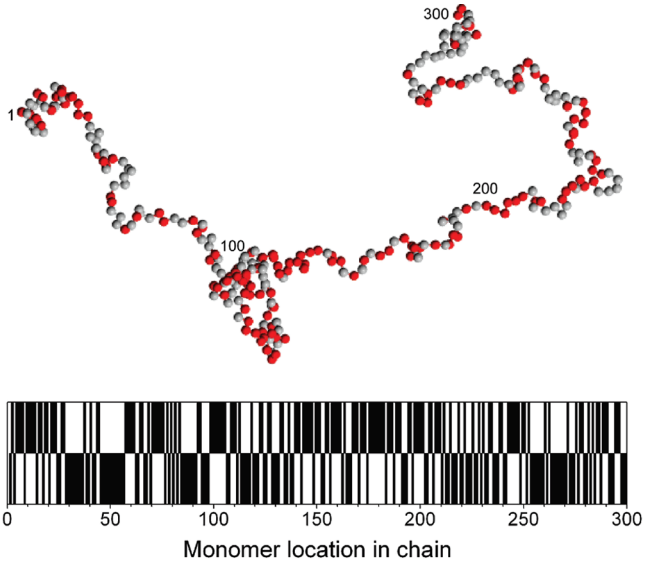

Figure 5. (top) Snapshot of the conformation of a $A_{0.5}B_{0.5}$ 300-mer at $kT/|\varepsilon_{AA}| = 8.0$ and R_{BA} ($= |\varepsilon_{BB}|/|\varepsilon_{AA}|$) = 0.50. The A and B units in the copolymer are depicted by gray and red balls, respectively. (bottom) Corresponding barcode plot for the same 300-mer.

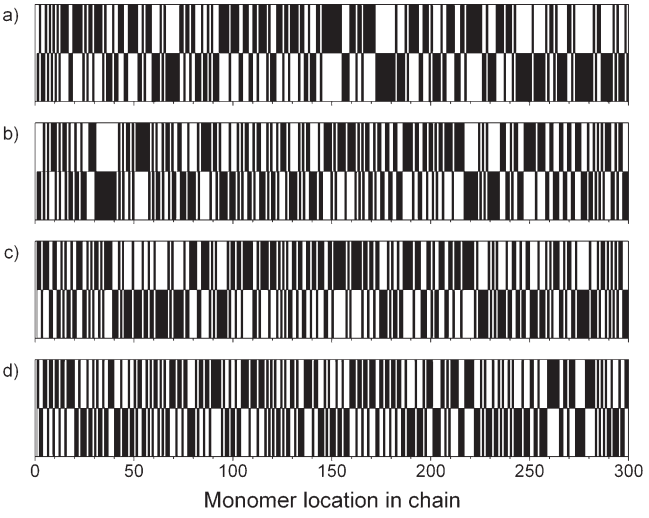

Figure 6. Barcode plots for $A_{0.5}B_{0.5}$ 300-mers at R_{BA} ($= |\varepsilon_{BB}|/|\varepsilon_{AA}|$) = 5.0 and $kT/|\varepsilon_{AA}|$ equal to (a) 0.2, (b) 0.6, (c) 0.8, and (d) 1.2.

Visual inspection of the data in Figure 6 reveals that while these polymers contain the same numbers of A and B, the distribution of A and B along the copolymer depends on the value of $kT/|\varepsilon_{AA}|$. To that end, the $kT/|\varepsilon_{AA}| = 0.2$ case shows a large number of wide white and black sections (blocky copolymer). At $kT/|\varepsilon_{AA}| = 0.6$, the strips are beginning to thin (i.e., the copolymer is becoming more random); further thinning occurs at $kT/|\varepsilon_{AA}| = 0.8$. Finally, at $kT/|\varepsilon_{AA}| = 1.2$, the barcode plot is composed mostly of thin strips, signifying a significant degree of randomness. Hence, the data reveal that one can effectively control the degree of randomness by simply varying $kT/|\varepsilon_{AA}|$.

In order to quantify the degree of randomness along $A_{1-x}B_x$ sequence, we slide a window of size λ monomers along the length of the chain, while counting the number of occurrences, $\gamma(\lambda)$, of a "1" within this window. (Alternatively we could count the occurrences of a "−1".) We define the dispersion of "1" as

$$D^2(\lambda) = \langle \gamma^2(\lambda) \rangle - \langle \gamma(\lambda) \rangle^2 \qquad (4)$$

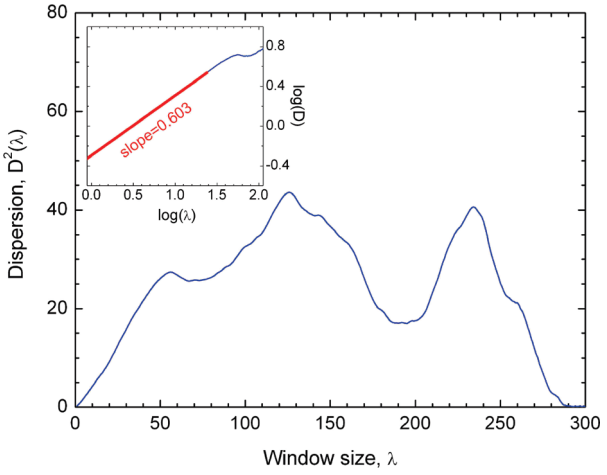

Figure 7. Dispersion plot for a 300-mer $A_{0.5}B_{0.5}$ at $kT/|\varepsilon_{AA}| = 0.2$ and R_{BA} ($= |\varepsilon_{BB}|/|\varepsilon_{AA}|$) $= 5.0$. The inset depicts a log(D)−log(λ) plot for the first 100 monomers of the chain.

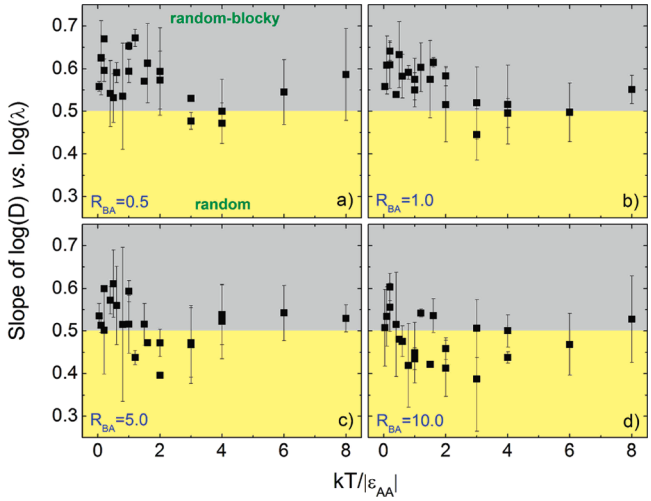

Figure 8. Slope of the log(D) vs log(λ) plot as a function of the reduced temperature ($kT/|\varepsilon_{AA}|$) for $A_{0.5}B_{0.5}$ 300-mers at R_{BA} ($= |\varepsilon_{BB}|/|\varepsilon_{AA}|$) equal to (a) 0.5, (b) 1.0, (c) 5.0, and (d) 10.0. The colored regions separate the random−blocky (gray) and random (yellow) comonomer sequences. The error bars were obtained by averaging over three simulation runs.

where dispersion is a general measure of the spread of the 1s along the length of the chain. For random copolymers, dispersion should be low or near zero (1s are spread evenly throughout the chain); for blocky copolymers, dispersion is high (1s are grouped together) and increases as chain length increases. The data in Figure 7 depict the dispersion, $D^2(\lambda)$, plotted as a function of window size, λ, ranging from $\lambda = 2$ to $\lambda = N$ (the entire length of the chain). It is known that the dispersion can be described by the power law $D(\lambda) \sim \lambda^{\alpha}$.[43] Accordingly, we select a sufficiently large fraction of the chain, say, the initial 1/4 of the chain, and plot log(D) vs log(λ).This plot, shown in the inset to Figure 7, for a 300-mer $A_{0.5}B_{0.5}$ at $kT/|\varepsilon_{AA}| = 0.2$ and $R_{BA} = 0.5$ gives a slope of 0.603. On the basis of the original work of Stanley and coworkers,[43] copolymers whose log(D) vs log(λ) slope is above 0.5 show long-range correlation, which is equivalent to "random−blocky" sequences. If the slope is smaller than 0.5 (i.e., no long-range correlation), we classify the copolymer as "random". This analysis of dispersion, $D^2(\lambda)$, is useful as shown in the data and discussion that follows.

We tested the effect of the parent homopolymer solubility and the B-solubility on the blockiness of copolymers by conducting multiple simulations at $kT/|\varepsilon_{AA}|$ ranging from 0.04 to 8.0 and various values of R_{BA}. Blockiness values were elucidated from the slope of log(D) vs log(λ) plots (cf. Figure 7). The resulting slopes for the 300-mers are presented in Figure 8. Four significant trends can be noted. First, decreasing the solubility of the B monomers (moving from Figure 8a to Figure 8d) decreases the blockiness of the $A_{0.5}B_{0.5}$ copolymers. For the case of good B solubility (cf. Figure 8a), most data lie in the random−blocky region. By comparison, for the case of poorest B solubility (cf. Figure 8d), most data lie in the random region. The increase in the randomness of the copolymer as the B solubility decreases is due to the inversion shown in Figures 3 and 4 which was discussed earlier. Second, for most R_{BA} values, the blockiness of the copolymer is not highest at the lowest reduced temperature ($kT/|\varepsilon_{AA}| = 0.04$) where the A solubility is the poorest; instead, the maximum blockiness value for all four sets occurs at $0.4 < kT/|\varepsilon_{AA}| < 1.2$. Obviously, a certain degree of insolubility (low $kT/|\varepsilon_{AA}|$) is required to promote coloring along the outer surface. However, near $kT/|\varepsilon_{AA}| = 0$ the coil is likely very tightly packed, which hinders its reorientation; newly formed B monomers cannot move aside to allow for coloring to occur at the adjoining monomer. Third, over the range of $kT/|\varepsilon_{AA}|$ from 1.0 to T^*_{θ} (≈3), increasing $kT/|\varepsilon_{AA}|$ promotes the randomness of the comonomer distribution. This trend is expected because the parent homopolymer is more likely to adopt coil-like conformations (cf. Figure 1), allowing coloring to occur along the length of the chain. Fourth, at values of $kT/|\varepsilon_{AA}|$ from $T^*_{\theta} \approx 3.0-8.0$, the comonomer distribution for most systems becomes slightly more blocky with increasing $kT/|\varepsilon_{AA}|$. The latter trend is somewhat surprising given that one would expect the randomness to increase with increasing $kT/|\varepsilon_{AA}|$. Apparently, while A is relatively coil-like, the difference in solubility of B relative to A causes pronounced changes in the coil conformation that result in increased random−blocky character of the comonomer sequences. For example, if one colors a parent chain initially at $kT/|\varepsilon_{AA}| = 8.0$ (good solubility) to $A_{0.5}B_{0.5}$ with $R_{BA} = 10.0$, $kT/|\varepsilon_{BB}|$ is 0.8 (poor solubility). Thus, there is an initial tendency of the copolymer to produce random sequences of A and B with increasing $kT/|\varepsilon_{AA}|$, but this is often followed by a reversal to random−blocky character with higher $kT/|\varepsilon_{AA}|$. In the following section, we will attempt to provide molecular insight into the observed high-$kT/|\varepsilon_{AA}|$ behavior.

The results discussed thus far indicate a clear trend: increasing $kT/|\varepsilon_{AA}|$ opens up the globule and allows the chain to adopt a coil-like conformation. While this situation is generally perceived to lead to more random comonomer distributions, decreasing the solubility of B may offset this effect by increasing the blockiness in the comonomer sequence along the chain. For instance, the data presented in Figure 8 indicate that for high $kT/|\varepsilon_{AA}|$ and most values of R_{BA}, the $A_{0.5}B_{0.5}$ copolymers exhibit an increased tendency to form random−blocky sequences upon increasing $kT/|\varepsilon_{AA}|$. More detail concerning the mechanism responsible for the formation of such copolymers can be elucidated by examining the copolymer conformations at various degrees of coloring. In Figure 9, we present snapshots of $A_{1-x}B_x$ conformations at increasing values of x (ranging from 0 to 0.5) for $kT/|\varepsilon_{AA}| = 4.0$ and $R_{BA} = 10.0$. Recall that $T^*_{\theta} \approx 3$ (cf. Figure 1). Initially, the A homopolymer adopts a coil-like conformation. As the coloring commences, the distribution of the B segments along $A_{1-x}B_x$ is initially random, up to $x \approx 0.2$. Further increase in the degree of coloring leads to a collapse of the chain at segments with high B population. This effect further intensifies as the reaction proceeds to higher degrees of coloring. The chain, while extended overall, now contains small globules at both chain ends that exhibit random−blocky character; these subglobules hold a high proportion of B monomers at an effective local solubility of $kT/|\varepsilon_{BB}| = 0.4$. Thus, despite the initial high-$kT/|\varepsilon_{AA}|$ conditions,

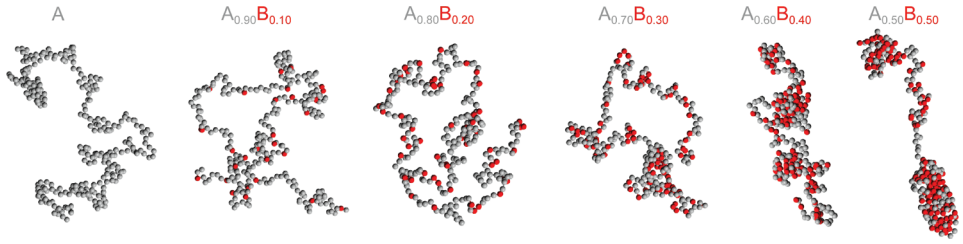

Figure 9. Conformations of $A_{1-x}B_x$ 300-mers at $kT/|\varepsilon_{AA}| = 4.0$ and R_{BA} ($= |\varepsilon_{BB}|/|\varepsilon_{AA}|$) = 5.0 at various degrees of coloring, x, ranging from 0 to 0.5. The A and B units in the copolymer are depicted by gray and red balls, respectively.

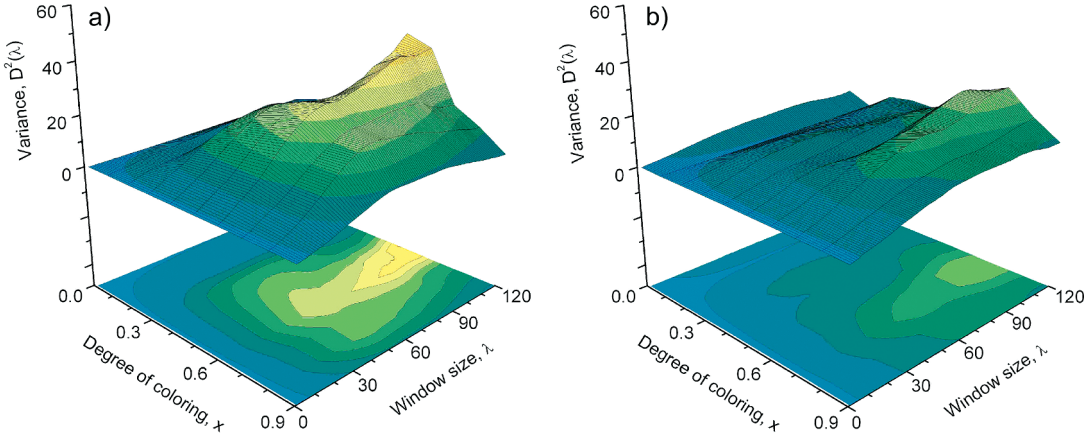

Figure 10. Dispersion as a function of the window size, λ, and degree of coloring, x, for $A_{1-x}B_x$ 300-mers at (a) $kT/|\varepsilon_{AA}| = 0.2$ and (b) $kT/|\varepsilon_{AA}| = 1.2$. Shown as 3-D plot and contour plot.

which generally promote a random distribution of B (and consequently A), the strong B−B interaction instead causes the chain to collapse and mimic low-$kT/|\varepsilon_{AA}|$ conditions which, in turn, results in an increased degree of blockiness of the B units. This picture also reveals that the blockiness in the comonomer distribution along the chain will likely not be uniform. There may be regions of higher randomness (i.e., in the middle of the chain) that coexist with regions of higher random−blocky character (i.e., the chain ends). This result also explains the rather large error bars in the log(D) vs log(λ) plots presented in Figure 8. Note that we have not attempted to further analyze the uniformity of the distribution of the sequences along the chain; this will be addressed in an upcoming publication.

From the previous discussions and the conformation snapshots presented in Figure 9, it is apparent that the conformation and the blockiness of the colored copolymer are a function of percent coloring. Up to this point, we have mainly considered the case $x = 0.5$, where the blockiness of the copolymer might be assumed to be at its highest possible value. The situation is more complex, however, prompting us to revisit the results in Figure 8 so as to stress the effect of the degree of coloring on the sequence distribution in $A_{1-x}B_x$ copolymers.

To investigate all values of x, in Figure 10 we plot $D^2(\lambda)$ as a function of both λ and the degree of coloring for $A_{1-x}B_x$ 300-mers for $R_{BA} = 5.0$ at $kT/|\varepsilon_{AA}|$ equal to (a) 0.2 and (b) 1.2 (we have included the corresponding contour plots as well.) Examination of the $kT/|\varepsilon_{AA}| = 0.2$ case (Figure 10a) reveals that the dispersion (and thus blockiness) in comonomer distribution increases with increasing degree of coloring, reaches a maximum at about 50−60% of coloring, and then decreases as one produces $A_{1-x}B_x$ copolymers with a large content of B. Turning now to the case of $kT/|\varepsilon_{AA}| = 1.2$ (Figure 10b), the situation changes dramatically. Starting from the A homopolymer, addition of B segments to the $A_{1-x}B_x$ copolymers does not seem to lead to any significant blockiness in A (or B) segments over the range $x = 0.0$ to $x = 0.3$. At this point, blockiness increases slightly and then remains relatively constant through the range of $0.3 < x < 0.6$ before increasing to a maximum blockiness around $x = 0.75$. We observe that the relationship between degree of coloring and blockiness in Figure 10b is not as smooth or direct as in Figure 10a and that coloring to $A_{0.5}B_{0.5}$ would not necessarily produce random copolymers with the highest degree of blockiness. It becomes apparent that the maximum blockiness values seen in Figure 8 might be improved upon by halting the coloring process at a lower degree or extending the process past $x = 0.5$. The latter point will be addressed in more detail in future work.

Conclusion

We provide molecular-level insight into recent experimental work on the bromination of parent homopolymer polystyrene in selected solvents. Discontinuous molecular dynamics simulation is employed to explore how the distribution of segments in A-*co*-B copolymers formed by "coloring" a homopolymer comprised of A-type monomers with a B chemical species depends on the system temperature, monomer solubilities, and extent of "coloring".[31] Here we have modeled the solubility of the monomers by adjusting the monomer−monomer interaction potential, ε_{ij}; for all unlike interactions, $\varepsilon_{AB} = 0$, and for like interactions, ε_{AA} and ε_{BB}, is varied. The solubility of the parent A-type homopolymer was varied by altering the system reduced temperature ($kT/|\varepsilon_{AA}|$), thereby regulating the initial polymer conformation prior to coloring. We simulated the "coloring" procedure for various combinations of $kT/|\varepsilon_{AA}|$ and $R_{BA} = |\varepsilon_{BB}|/|\varepsilon_{AA}|$ and examined how the polymer conformation and resulting sequence depended on the degree of "coloring", x. We stress several trends observed and reported on in this study. First, increasing $kT/|\varepsilon_{AA}|$ leads to a decrease in blockiness in the comonomer distribution; exceptions to this trend are discussed. Second, increasing the degree of "coloring" also decreases blockiness. Lastly, we detect increased "random−blocky" character of the resultant $A_{1-x}B_x$ copolymer

upon decreasing the solubility of the B species (expressed here in terms of $R_{BA} = |\varepsilon_{BB}|/|\varepsilon_{AA}|$). Some counterintuitive trends were found, however. For instance, it was shown that poor B solubility initially causes the copolymer to swell as B monomers move into the globule away from the solvent. We also demonstrated that when the parent homopolymer is soluble but the colored monomer is highly insoluble ($kT/|\varepsilon_{BB}| < T_\theta$), the resulting copolymer can be blocky due to the formation of subglobules. These results and discussion could guide experimenters in developing copolymers with specific A−B patterning, allowing them to tailor-make copolymers for further research into miscibility, surface adsorption, and other research areas.

While this present work provides important insight into the coloring process, much more needs to be done in order to fully comprehend the role of the molecular interactions as well as the role of the different rate phenomena on the transformation of homopolymers into copolymers via selective chemical coloring. For instance, it is of vital importance to address the time scales involved in the rearrangement of the parent macromolecule and the mobility of the diffusing species. This and other related topics will be the subject of future publications.

Acknowledgment. This work was supported by the National Science Foundation under Grants DMR-0353102 and OISE-0730243 awarded to J.G. and the Office of Energy Research, Office of Basic Sciences, Chemical Science Division of the U.S. Department of Energy, under Grant DE-FG05-91ER14181 awarded to C.K.H. We thank Ravish Malik for helpful discussions.

References and Notes

(1) Balazs, A. C.; Gempe, M. *Macromolecules* **1991**, *24*, 167–176.
(2) Chai, Z.K.; Sun, R.N.; Karasz, F. E. *Macromolecules* **1992**, *25*, 6113–6118.
(3) Angerman, H.; Hadziioannou, G.; ten Brinke, G. *Phys. Rev. E* **1994**, *50*, 3808–3813.
(4) Smith, G. D.; Russell, T. P.; Kulaserke, R.; et al.et al. *Macromolecules* **1996**, *29*, 4120–4124.
(5) Simmons, E. R.; Chakraborty, A. K. *J. Chem. Phys.* **1998**, *109*, 5493–5496.
(6) Bernard, B.; Brown, H. R.; Hawker, C. J.; et al.et al. *Macromolecules* **1999**, *32*, 6254–6260.
(7) Eastwood, E. A.; Dadmun, M. D. *Macromolecules* **2002**, *35*, 5069–5077.
(8) Montanari, A.; Mueller, M.; Mezard, M. *Phys. Rev. Lett.* **2004**, *92*, 185509.
(9) Khokhlov, A. R.; Berezikin, A. V.; Khalatur, P. G. *J. Polym. Sci., Part A* **2002**, *42*, 5339.
(10) Khokhlov, A. R.; Khalatur, P. G. *Curr. Opin. Colloid Interface Sci.* **2004**, *8*, 3 and references therein.
(11) Khokhlov, A. R.; Khalatur, P. G. *Curr. Opin. Colloid Interface Sci.* **2005**, *10*, 22 and references therein.
(12) Khalatur, P. G.; Khokhlov, A. R. *Prog. Polym. Sci.* **2006**, *196*, 1 and references therein.
(13) Lozinsky, V. I. *Prog. Polym. Sci.* **2006**, *196*, 87 and references therein.
(14) Zhang, G.; Wu, C. *Prog. Polym. Sci.* **2006**, *196*, 101.
(15) Faldi, A.; Genzer, J.; Composto, R. J.; Dozier, W. D. *Phys. Rev. Lett.* **1995**, *74*, 3388.
(16) Genzer, J.; Composto, R. J. *Macromolecules* **1998**, *31*, 870.
(17) Pellegrini, N. N.; Sikka, M.; Satija, S. K.; Winey, K. I. *Polymer* **2000**, *41*, 2701–2704.
(18) Kulasekere, R.; Kaiser, H.; Anker, J. F.; Russell, T. P.; Brown, H. R.; Hawker, C. J.; Mayes, A. M. *Macromolecules* **1996**, *29*, 5493–5496.
(19) Benkoski, J. J.; Fredrickson, G. H.; Kramer, E. J. *J. Polym. Sci., Part B: Polym. Phys.* **2001**, *39*, 23632377.
(20) Mansky, P.; Liu, Y.; Huang, E.; Russell, T. P.; Hawker, C. *Science* **1997**, *275*, 1458–1460.
(21) Moghaddam, M. S.; Chan, H. S. *J. Chem. Phys.* **2006**, *125*, 164909.
(22) For a recent review see : Khalatur, P. G.; Khokhlov, A. R. *Adv. Polym. Sci.* **2006**, *195*, 1 and references therein.
(23) Bratko, D.; Chakraborty, A. K.; Shakhnovich, E. I. *Chem. Phys. Lett.* **1997**, *280*, 46–52.
(24) Chakraborty, A. K.; Golumbfskie, A. J. *Annu. Rev. Phys. Chem.* **2001**, *52*, 537–573.
(25) Chakraborty, A. K. *Phys. Rep.* **2001**, *342*, 2–61.
(26) Khokhlov, A. R.; Khalatur, P. G. *Physica A* **1998**, *249*, 253–261.
(27) Khokhlov, A. R.; Khalatur, P. G. *Phys. Rev. Lett.* **1999**, *82*, 3456–3459.
(28) Lozinskii, V. I.; Simenel, I. A.; Kurskaya, E. A.; et al.et al. *Dokl. Chem.* **2000**, *375*, 273–276.
(29) Semler, J. J.; Genzer, J. *J. Chem. Phys.* **2006**, *125*, 014902.
(30) Semler, J. J.; Jhon, Y. K.; Tonelli, A.; Beevers, M.; Krishnamoorti, R.; Genzer, J. *Adv. Mater.* **2007**, *19*, 2877.
(31) Jhon, Y. K.; Semler, J. J.; Genzer, J. *Macromolecules* **2008**, *41*, 6719.
(32) Han, J.; Jeon, B. H.; Ryu, C. Y.; Semler, J. J.; Jhon, Y. K.; Genzer, J. *Macromol. Rapid Commun.* **2009**, *30*, 1543.
(33) Jhon, J. K.; Krishnamoorti, R.; Genzer, J. Manuscript in preparation.
(34) Strickland, L. A.; Hall, C. H.; Chvosta, J.; Genzer, J. Manuscript in preparation.
(35) Smith, S. W.; Hall, C. K.; Freeman, B. D. *J. Comput. Phys.* **1997**, *134*, 16.
(36) Rapaport, D. C. *J. Phys. A: Math. Gen.* **1978**, *11*, L213.
(37) Rapaport, D. C. *J. Chem. Phys.* **1979**, *71*, 3299.
(38) Bellemans, A.; Orban, J.; Belle, B. V. *Mol. Phys.* **1980**, *39*, 781.
(39) Andersen, H. C. *J. Chem. Phys.* **1980**, *72*, 2384.
(40) Strickland, L. A.; Hall, C. K.; Genzer, J., submitted for publication.
(41) Szleifer, I.; O'Toole, E. M.; Panagiotopoulos, A. Z. *J. Chem. Phys.* **1992**, *97*, 6802.
(42) Rissanou, A. N.; Anastasiadis, S. H.; Bitsanis, I. A. *J. Polym. Sci., Part B: Polym. Phys.* **2006**, *44*, 3651.
(43) Peng, C. K.; Buldyrev, S. V.; Goldberger, A. L.; et al.et al. *Nature* **1992**, *356*, 168.